

# Allele surfing promotes microbial adaptation from standing variation

## Appendix B: Additional experimental results

Matti Gralka<sup>1</sup>, Fabian Stiewe<sup>2</sup>, Fred Farrell<sup>3</sup>, Wolfram Möbius<sup>1</sup>, Bartek Waclaw<sup>3,4</sup>, and Oskar Hallatschek<sup>1</sup>

<sup>1</sup>*Departments of Physics and Integrative Biology, University of California, Berkeley, CA 94720*

<sup>2</sup>*Biophysics and Evolutionary Dynamics Group, Max Planck Institute for Dynamics and Self-Organization, 37077 Göttingen, Germany*

<sup>3</sup>*SUPA, School of Physics and Astronomy, University of Edinburgh, Mayfield Road, Edinburgh EH9 3JZ, United Kingdom*

<sup>4</sup>*Centre for Synthetic and Systems Biology, The University of Edinburgh*

### Short description of figures

B1	Selective advantages as function of drug concentration and comparison between liquid culture and colliding colony measurements. . . . .	2
B2	Increase in mean fitness during range expansion and uniform growth to same final population size. . . . .	2
B3	Dependence of sector number on initial mutant frequency and selective advantage. . . . .	3
B4	Probability that no sectors exist at the front for different initial mutant frequencies and selective advantages. . . . .	3
B5	Two regimes of yeast colony radius growth. . . . .	4
B6	Number of sectors for different number of cells in inoculum. . . . .	5
B7	Frequency per sector for <i>E. coli</i> compared to <i>S. cerevisiae</i> colonies. . . . .	6
B8	Tracking of individual cell dynamics in <i>S. cerevisiae</i> and <i>E. coli</i> population fronts. . . . .	7
B9	Overall front speed and speed of individual cells at and behind the front for <i>S. cerevisiae</i> . . . . .	8
B10	Change of a cell's distance to the front as a function of time. . . . .	9

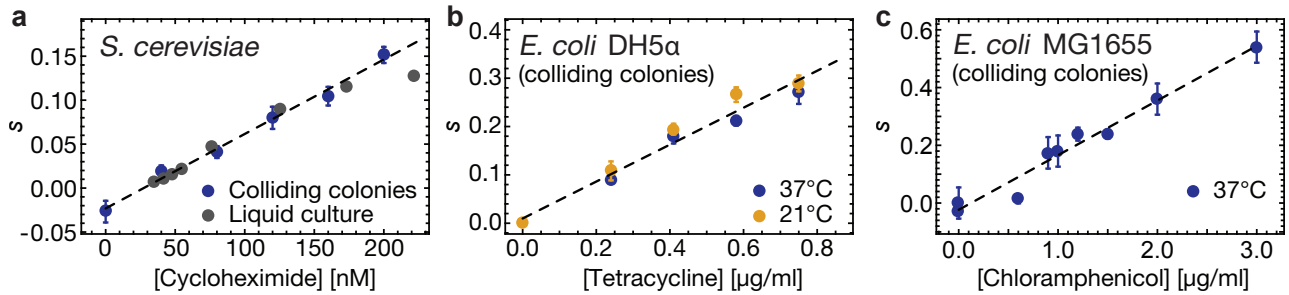


Figure B1: Selective advantages  $s$  between resistant and sensitive strains as function of drug concentration for *S. cerevisiae* and *E. coli* for different assays and conditions. (a) Budding yeast strains with W303 background (yMM9 and yJHK111) used in Fig. 1. Best linear fit is shown and used throughout the paper. Liquid culture fitness measurements (3 replicates from the same initial culture per data point, gray dots) over 60 generations agree with the colliding colony result (blue dots) for a range of cycloheximide concentrations. (b) *E. coli* DH5 $\alpha$  competition (strains eOH2 and eOH3) on plates with different concentrations of tetracycline at 37°C (blue data points) and 21°C (yellow data points) using the colliding colony assay. Temperature had no significant impact on the relative fitness of the two strains. Best fit is shown through combined data and used throughout the paper. (c) *E. coli* strain MG1655 competed against strain SJ102 at different concentrations of chloramphenicol, measured using the colliding colony assay, with linear best fit. All error bars are standard error of the mean (about 20 replicates per data condition, except for well-mixed competition).

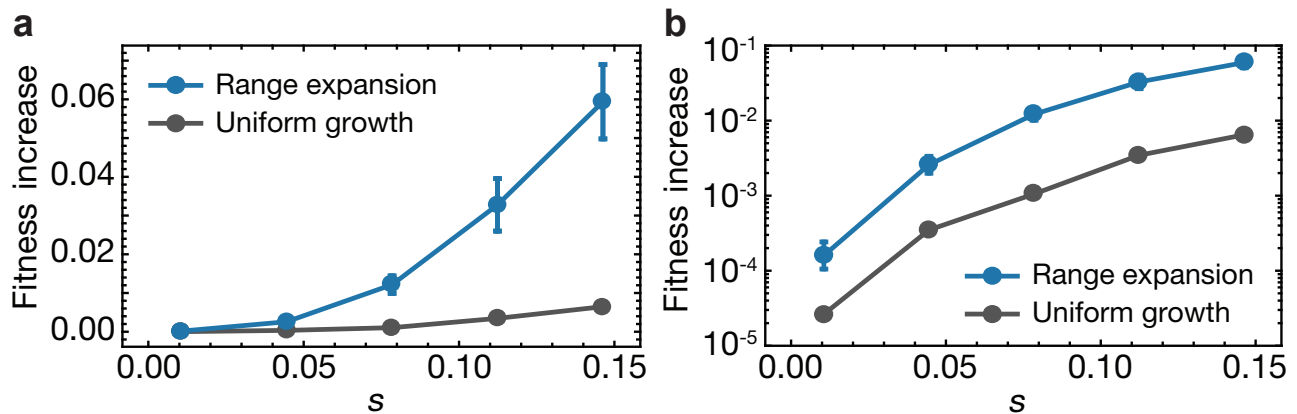


Figure B2: Increase in mean fitness, defined as  $\overline{\Delta W} = (P_f - P_1)s$ , computed from the final mutant frequency  $P_f$  measured in Fig. 1h, with linear (a) and logarithmic axis (b). Range expansions leads to a higher increase in mean fitness than uniform growth to the same final population size.

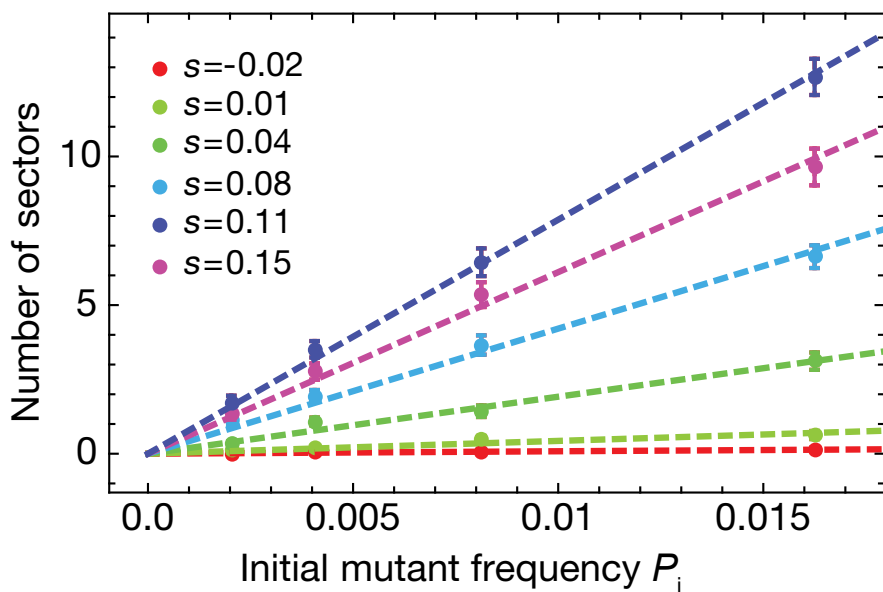


Figure B3: Number of sectors  $N_{\text{sec}}$  counted in yeast colonies at different initial mutant frequencies  $P_i$  and selective advantages  $s$ . The proportionality of sector number and initial mutant frequency implies that sectors arise independently for small enough fractions. Points are averages from 30 colonies per condition, error bars correspond to the standard error of the mean.

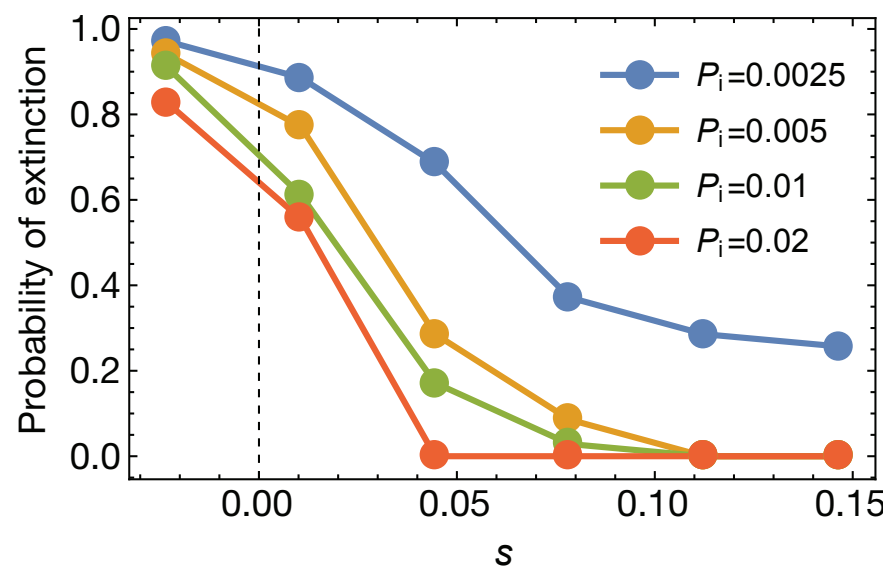


Figure B4: Probability of extinction, defined as the probability of having zero sectors at the front, in yeast colonies for a variety of initial mutant frequencies  $P_i$  and selective advantages  $s$  (35 colonies from same initial culture per data point).

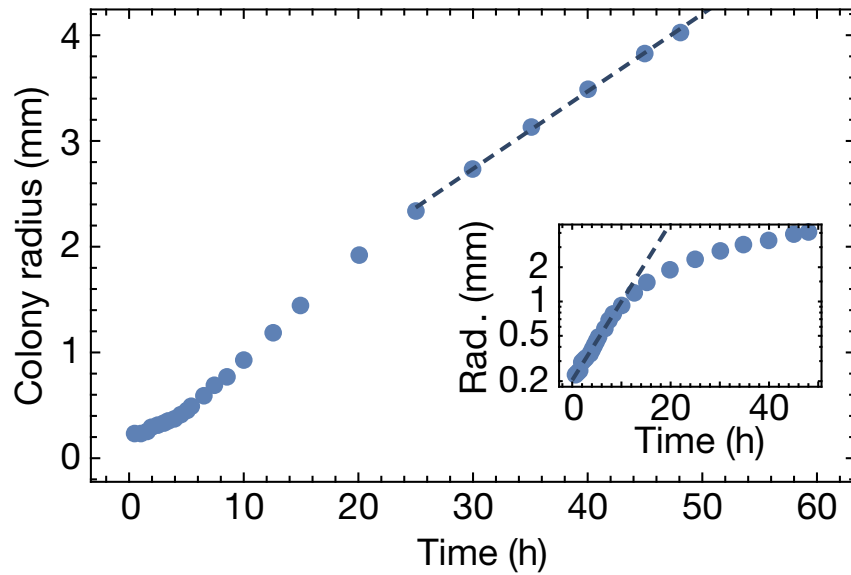


Figure B5: Two regimes of yeast colony radius growth. Colony radii extracted from a time lapse movie of a growing yeast colony. Single yeast cells were inoculated onto an agar plate and grown for about 12 hours. Once microcolonies were detectable, the agar plate was transferred to a stage-top incubator and the colony was imaged in bright-field and fluorescence light every 30 minutes. Initially, the colony radius growth exponentially, indicating that the radius of the colony is not yet larger than the eventual growth layer thickness of the colony. For late times, the colony radius grows linearly in time, which can be interpreted as a growth layer of constant final thickness.

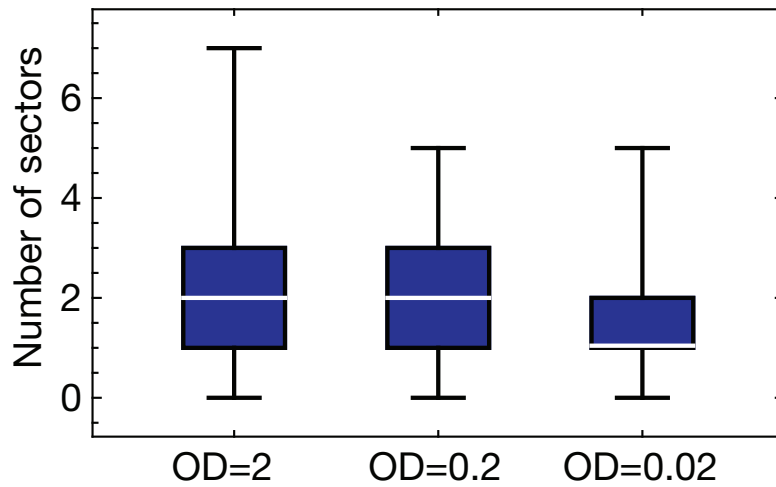
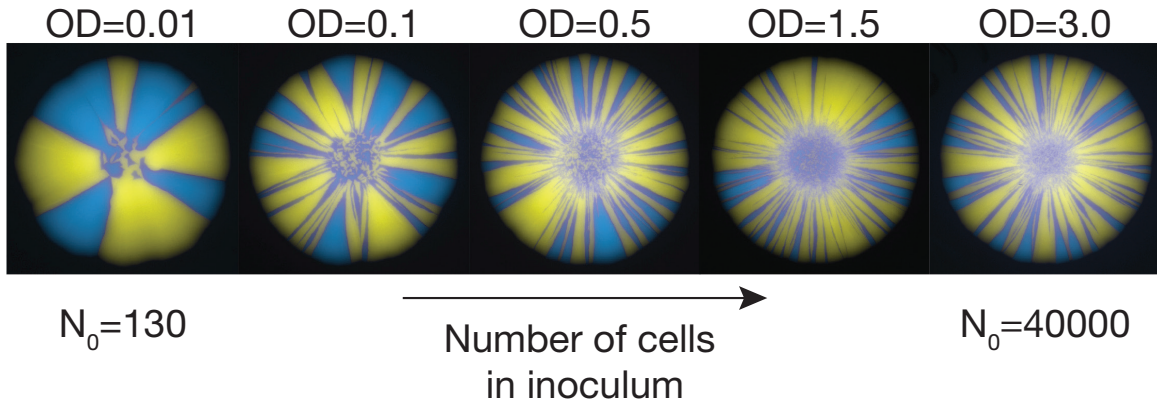


Figure B6: Number of sectors for different number of cells in inoculum. Top: Example images show the change of population patterning with increasing cell number in the inoculum. Here, we mixed two selectively neutral *S. cerevisiae* strains (yJHK111 and yJHK112) at an initial ratio of  $P_1 = 0.5$ . For large cell number  $N_0$  the population pattern does not change when increasing  $N_0$  further. (Bottom) Number of sectors measured in standing variation assays for different inocula, for the same strains. We assayed 50 neutral colonies with an initial ratio of  $P_1 = 0.01$  per dilution, allowing us to count individual sectors. We found no significant difference in sector numbers when diluting a typical culture (OD=2 in the figure, corresponding to about 30000 cells in a  $2\mu\text{l}$  droplet) by a factor of 10 ( $p > 0.05$ , Mann-Whitney U-test). Dilution by another factor of 10 showed again no significant difference to the intermediate case (first 10-fold dilution), but did show a significant difference ( $p < 0.05$ ) to the original case. Taken together we conclude that the number of sectors is not sensitive to density of the initial culture, given that the inoculum contains at least about 1000 cells in a  $2\mu\text{l}$  droplet. This means that typical pipetting errors or a small change in cell densities of the culture mixtures, which we estimate to be in the range of at most 10 per cent, should have no impact on the number of sectors. The observations can be understood from Fig. 3: Only cells at the front have a chance to surf, and in our experiments, the front is imposed as an initial condition by the drying inoculum. Hence, as long as the cells in the droplet form a continuous ring of cells (such that at every point of the ring there is a defined front), the number of cells in the bulk of the inoculum plays no role in the future fate of the colony.

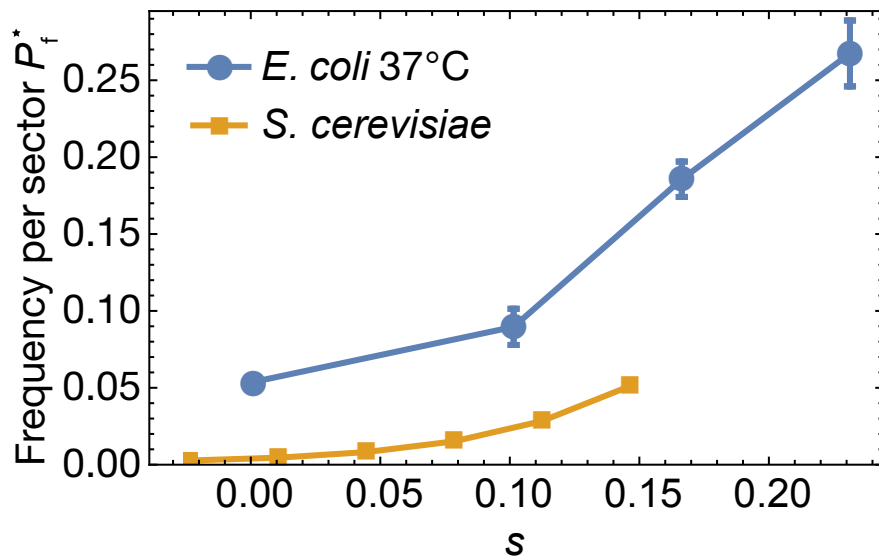


Figure B7: Frequency per sector for *E. coli* DH5 $\alpha$  grown at 37°C (blue dots, see also Fig. 4f) together with corresponding data for *S. cerevisiae* (data as in Fig. 1j). Only individual, non-interacting sectors were selected for analysis. Each individual sector is much larger in (relative) size in *E. coli* than in *S. cerevisiae* colonies. In fact, a yeast sector at the highest assayed selective advantage has a relative size comparable to a neutral *E. coli* sector. Error bars are standard errors of the mean, from about 20 sectors per selective advantage  $s$ .

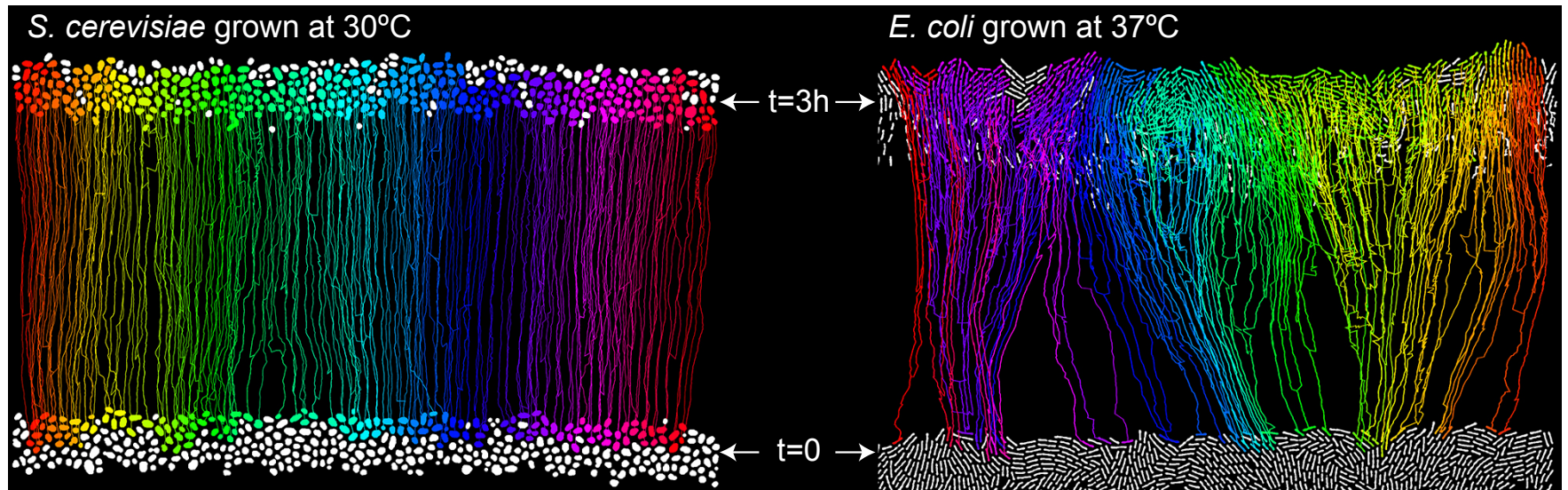


Figure B8: Tracking of individual cell dynamics in *S. cerevisiae* and *E. coli* front reveal microscopic motion patterns. *S. cerevisiae* and *E. coli* fronts tracked for 3 hours (full images from Fig. 3). Shown are the front of each colony at the start of the experiment ( $t=0$ ) and after 3 hours. All tracked lineages and cells are colored. White cells at the top could not be tracked, while white cells at the bottom have no tracked descendants at the front after 3 hours.

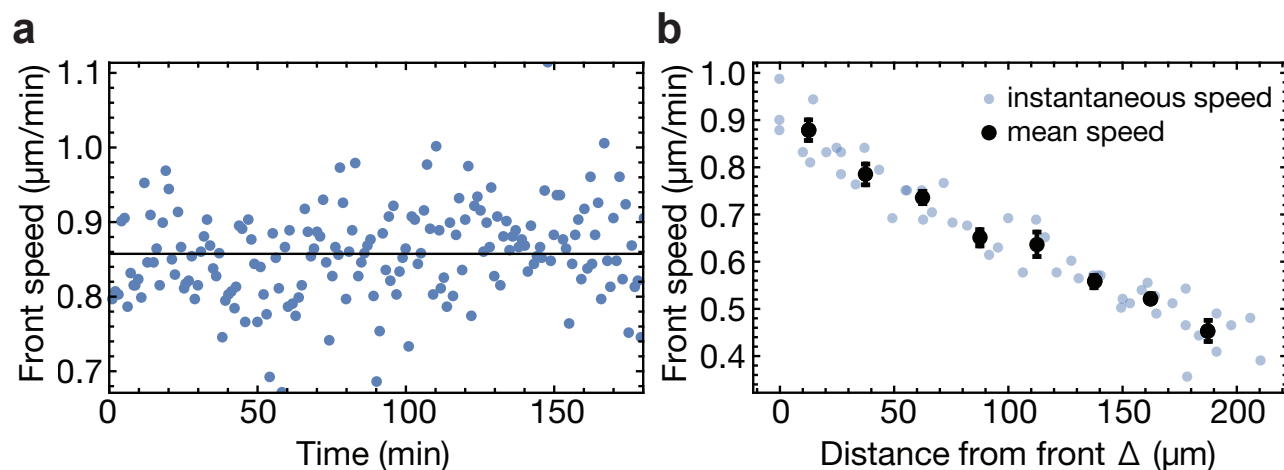


Figure B9: Overall front speed and speed of individual cells at and behind the front for *S. cerevisiae*. A. Instantaneous front speed, defined as the difference in mean front position in each frame, and time average (solid line). The front speed in a *S. cerevisiae* colony is constant over at least three hours (from SI movie 1, see also Fig. B5). B. Speed of individual cells as a function of distance from the front. Speed was measured by visually following 16 individual cells, initially a distance  $\Delta$  behind the front, and recording their position every 30 minutes for 90 minutes. Instantaneous speed was computed by dividing the relative change in position by 30 minutes. Here,  $\Delta$  is the distance from the front at the beginning of each 30 minute interval. For the mean speed, data were binned in  $25\mu\text{m}$  intervals. An approximately linear decrease in speed implies near-constant growth rate at least  $200\mu\text{m}$  into the bulk of the colony.



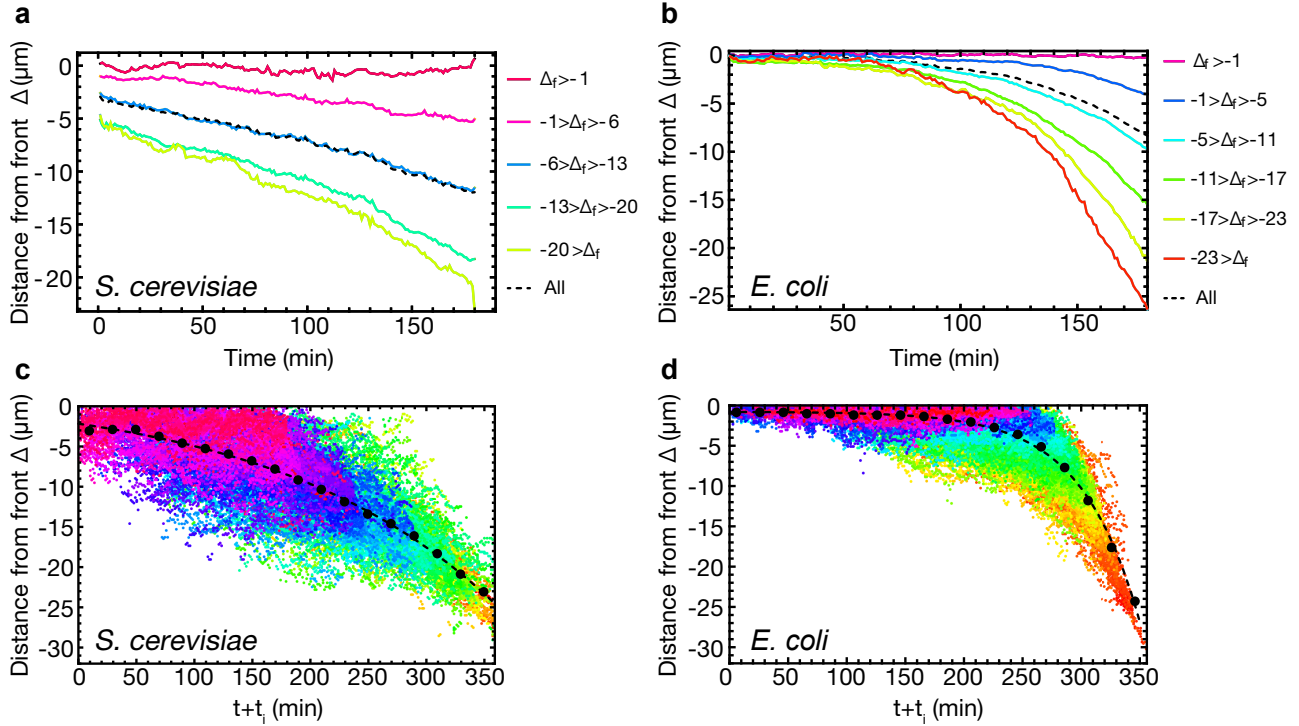


Figure B10: Dynamics of lineages at and behind the front, extracted from SI movies 1 and 2, for *S. cerevisiae* and *E. coli*. Front position was recorded at every time point, and the distance to the front computed for all cells. For (a) & (b), cell trajectories were pooled together depending on their final distance  $\Delta_f$  from the front at the end of the movies (see color legends). Over time, all cells falls behind the front on average, except those that remain directly at the front until the end (for these cells,  $\Delta_f > -1$ ).

To understand the dynamics of cells falling behind the front, we assumed that exterior parameters did not change over the course of the experiment and that therefore, only time differences should matter. This would imply that at any given time, the distance from the front should determine future dynamics (except for cells directly at the front). In (c) and (d), we show the distance  $\Delta$  from the front of each cells (color scheme as in (a) and (b), respectively), shifted such that the final distances  $\Delta_f$  from the front of each cell's trajectory overlapped with the cell trajectory with the largest  $\Delta_f$  (shown in red). Binning over intervals of 20 minutes reveals the average dynamics of cells falling behind the front (black dots): the distance  $\Delta$  to the front increases exponentially (fit, dashed line) in time, independently of position, except for cell that "surf", i.e., stay at the front for the full duration of the experiment, shown in magenta.

From the shifted cell trajectories, we extracted the histograms of initial distance to the front of cells, conditional on surfing. For the histograms in Fig. 3, we pooled cell trajectories with  $t + t_i < 10\text{min}$  and  $t + t_i < 75\text{min}$  for *S. cerevisiae* and *E. coli*.